Relationship Between Morphology and Micromechanical Toughening Mechanisms in Modified Polypropylenes

G.-M. KIM,[1] G. H. MICHLER,[1,*] M. GAHLEITNER,[2] and J. FIEBIG[2]

[1]Department of Materials Science, Martin-Luther-University Halle-Wittenberg, D-06217 Merseburg, Germany, and
[2]PCD Polymere GmbH A-4021, Linz, Austria

SYNOPSIS

Deformation and fracture processes of two types of modified polypropylenes (PPs) were investigated *in situ* by high voltage electron microscopy (HVEM, 1 MV) and scanning electron microscopy (SEM). One type of PP modified with ethylene–propylene block copolymer rubber (EPR) showed a variation in particle size and interparticle distance with content of ethylene. In the other series of modified PP, Al_2O_3 filler particles with concentrations of 10 and 60 wt % were used. The micromechanical toughening mechanism was comparable in both types. Deformation structures in both systems are closely connected with cavitation and void formation: the systems modified with EPR show void formation inside the modifier particles; in the systems modified with Al_2O_3, debonding occurs at the interface between the particles and the matrix. Additionally, the effect of the morphology of the modifier particles on micromechanical deformation processes was studied. The experiments showed that besides particle size and center-to-center distance between particles, the ratio of center-to-center distance to particle diameter plays an important role. Models (three-stage mechanism) for the micromechanical deformation process are proposed. © 1996 John Wiley & Sons, Inc.

INTRODUCTION

Toughness is a very important property for many applications of materials. A profound understanding of the relationship between the morphology and deformation properties of polymers is important for the development of polymer systems with improved impact toughness. To improve toughness of a polymeric material, various modifier particles with different physical properties can be added to the polymeric matrix.[1] It is known that the modifier particles in the matrix act as stress concentrators of the applied stress.[2] In such a modified polymer the plastic deformation process shows either craze formation, shear band formation, or shear yielding around the modifier particles. It is closely connected with cavitation.

Recently, many investigations have been done on the influence of the modifier particle size and its size distribution on the micromechanical toughening mechanisms such as crazing, shear yielding, and formation of dilatational bands, etc. Wu[3] investigated the deformation mechanism of nylon/ethylene–propylene block copolymer rubber (EPR) systems and revealed the decisive role of the surface-to-surface interparticle distance for toughness. Other concepts of rubber-toughening mechanisms were suggested by Borggreve et al.[4] and Hobbs et al.[5] for nylon/EPR systems and by Sue and Yee[6] for nylon/poly(phenylene oxide) rubber systems. They proposed that cavitation or void formation within rubber particles or at the interface plays an important role in the toughening mechanism. However, there is still much controversy regarding the appropriate concepts for the explanation of the toughening mechanisms. It is now generally accepted that there are two categories of toughening mechanisms in disperse systems: the energy is absorbed mainly by formation of crazes at the rubber particles (multiple crazing) as in high-impact polystyrene (HIPS) and numerous grades of acrylonitrile–butadiene–styrene polymers (ABS)[1,7–9]; or the energy is absorbed

* To whom correspondence should be addressed.

Journal of Applied Polymer Science, Vol. 60, 1391–1403 (1996)
 CCC 0021-8995/96/091391-13

Table I Mechanical Properties from Uniaxial Tensile Tests, Notched Izod-Impact (Charpy) Tests, and Structural Parameters from SEM

Material	Ethylene Content (Mol %)	Tensile Modulus, E (MPa)	Notched Izod-Impact Charpy (kJ/m²) +23°C	Notched Izod-Impact Charpy (kJ/m²) −20°C	D (μm)	CD (μm)	CD/D	Morphology of EPR Particle	Deformation
Sample 1	6	880	28.9	1.7	0.3	2.0	6.7	Only one PE inclusion with EP-rubber shell	Shear yielding
Sample 2	20	1030	34.0	6.7	1.6	3.7	2.3	Several PE inclusions with EP-rubber shell	Crazelike

D, particle diameter; CD, center-to-center distance; CD/D, ratio.

through shear yielding between the modifier particles (multiple shear yielding) as in impact modified polyamide (PA) and impact modified PP.[4,8,10]

In general, the addition of rubber particles favors the increase of toughness, whereas inorganic filler particles are added in an attempt to improve the stiffness. It has been found that micromechanical deformation processes in particle filled thermoplastics are very similar to processes in rubber modified polymers.[11]

In detail, micromechanical deformation processes are studied in relation to the type of modifier particle, the internal morphology of modifier particles, and the ratio of center-to-center distance to particle size. Several different techniques of electron microscopy, including transmission (TEM), scanning (SEM), and high voltage electron microscopy (HVEM) were used to investigate these dependencies in both types of modified PPs.

EXPERIMENTAL

Materials

Two different kinds of modified PPs were chosen: PP modified with EPR and PP modified with Al_2O_3 filler particles.

Two different samples of EPR modified PP are so-called "reactor blends" produced in a two-stage polymerization process similar to those described in literature.[12,13] The matrix phase is produced here in the first reactor in liquid propylene, while the EPR phase is produced in a second reactor in the gas phase. As the EP copolymerization taking place in the second reactor is a statistical process leading to a mixture of the crystalline and amorphous phases, no exact quantification of EPR is possible; therefore, only the quantity of ethylene is given in the characterization. To investigate the effects of particle size and center-to-center distance on the micromechanical toughening mechanisms, samples are produced by different contents of ethylene. They are defined as follows:

- Sample 1: EPR with small particle diameter (average particle D = 0.3 μm) and large ratio of center-to-center distance (CD) and particle diameter (D).
- Sample 2: EPR with large particle diameter (average particle diameter D = 1.58 μm) and small ratio of CD/D.

The detailed quantities are listed in Table I.

Particle-filled PP was modified with Al_2O_3 particles, one sample containing 10 wt % (sample 3) and the other sample 60 wt % (sample 4). In both samples the average filler particle size was about 1 μm.

Study of Morphology

To study the morphology, three preparation and investigation techniques were used. The rubber phase of the samples was chemically selectively stained with chlorosulfonic acid and osmium tetroxide or ruthenium tetroxide. Ultrathin sections about 0.1 μm thick were microtomed at −80°C and investigated in a conventional TEM. Semithin sections (up to a few microns thick) were prepared by ultramicrotomy at −80°C. They were studied with 1000 kV HVEM, revealing clearly larger particles and thus showing the true particle diameter distribution. Brittle fracture surfaces were prepared at low temperature and investigated by SEM showing preferentially larger particles.

In the samples of EPR modified PP, the particle size, its size distribution, and center-to-center distance were determined using SEM micrographs from

low temperature fractured surfaces. For the samples of Al_2O_3 modified PP, they were directly measured from HVEM micrographs with the help of a computerized image analyzer.

Micromechanical Deformation Processes

To get an overview about deformation processes, dumbbell-shaped specimens were strained with a rate of 0.5 mm/min at 23°C and studied by light microscopy during the tensile tests. For getting detailed information, samples were deformed and investigated *in situ* by 1-MV HVEM and SEM. All deformation tests under the microscope were performed at room temperature. The specimens for HVEM and SEM investigations were microtomed at −80°C with a thickness of about 1 μm for EPR modified PP and a thickness of about 2 μm for Al_2O_3 particle filled PP.

RESULTS

Morphology

There are morphological differences in the systems with EPR modification. Figure 1(a) shows a TEM micrograph of sample 1. Figure 1(b) is taken from sample 2. Micrographs show that the rubber particles are well dispersed in the PP matrix. In phase structure three characteristics are clearly visible: the matrix of semicrystalline PP containing lamellae; a structureless region around the particles, which consists of an amorphous ethylene–propylene rubbery phase (this region appears dark); and inclusions in the particles, which consist of semicrystalline polyethylene (PE).

The differences between sample 1 and sample 2 consist of the size and internal structure of the particles: in sample 1 the EPR particles possess only one PE inclusion, whereas there are several PE inclusions in sample 2.

Figure 2 shows typical HVEM micrographs of the PP systems modified with Al_2O_3 revealing the particles dispersed in the PP matrix.

TEM micrographs of ultrathin sections are not well suited to determine true particle size, particle size distribution, and center-to-center distance because ultrathin sections usually contain only very few particles. Therefore, the quantitative characterization of dispersed particles was performed by use of SEM. At liquid nitrogen temperature fracture surfaces, spherical rubber particles were revealed, counted, and measured to determine particle size, particle size distribution, and center-to-center distance between the particles for the individual blends. The results are summarized in Table I.

Micromechanical Deformation Processes

PP Modified with EPR Particles

Figure 3 shows HVEM micrographs taken during deformation of sample 1 modified with small size EPR particles. In the early stage of the deformation process (this process occurs as soon as the deviation of the elastic line to the yield point in the stress–strain curve in the tensile test, about 20%), EPR particles deform together with the matrix [Fig. 4(a)]. Void formation (cavitation) appears suddenly in the plastically deformed EP rubbery shell [Fig. 4(b)]; then the voids grow gradually with the increasing strain. Particles as well as the adjacent matrix are strongly plastically deformed (elongation up to 900%). Together with void formation and particle elongation, weak shear bands form in the matrix between particles (see Fig. 3). With increasing strain, a more intense shear deformation appears between particles/voids. Therefore, shear flow in the matrix appears either as shear bands or as diffuse shear yielding.

Figure 5 shows HVEM micrographs taken during deformation of sample 2 modified with large size particles. A well-developed fibrillar deformation structure appears, which resembles a crazelike deformation structure. To study the deformation processes at the beginning of deformation, *in situ* experiments were performed with the scanning electron microscope (Fig. 6). In the early stage of deformation, stress concentration takes place around the EPR particles. After this, EPR particles deform simultaneously with the PP matrix [Fig. 6(a)] and void formation occurs predominantly in the EPR particles at the interface of EP inclusions [Fig. 6(b)]. With increasing applied stress, the number and size of the voids increase simultaneously. However, if the applied stress reaches the maximum tensile strength of the sample, the number of voids appears to be constant, but the size of the voids continues to increase. By further increasing the strain, the voids begin to interact with each other as shown in Figure 6; simultaneously, the shear yielding of the matrix takes place.

Figure 7 shows an SEM micrograph of a low temperature fracture surface of the region of the tensile specimen where the stress whitening appeared during the uniaxial tensile test. Void formation due to cavitation localized at the particle/matrix interfaces

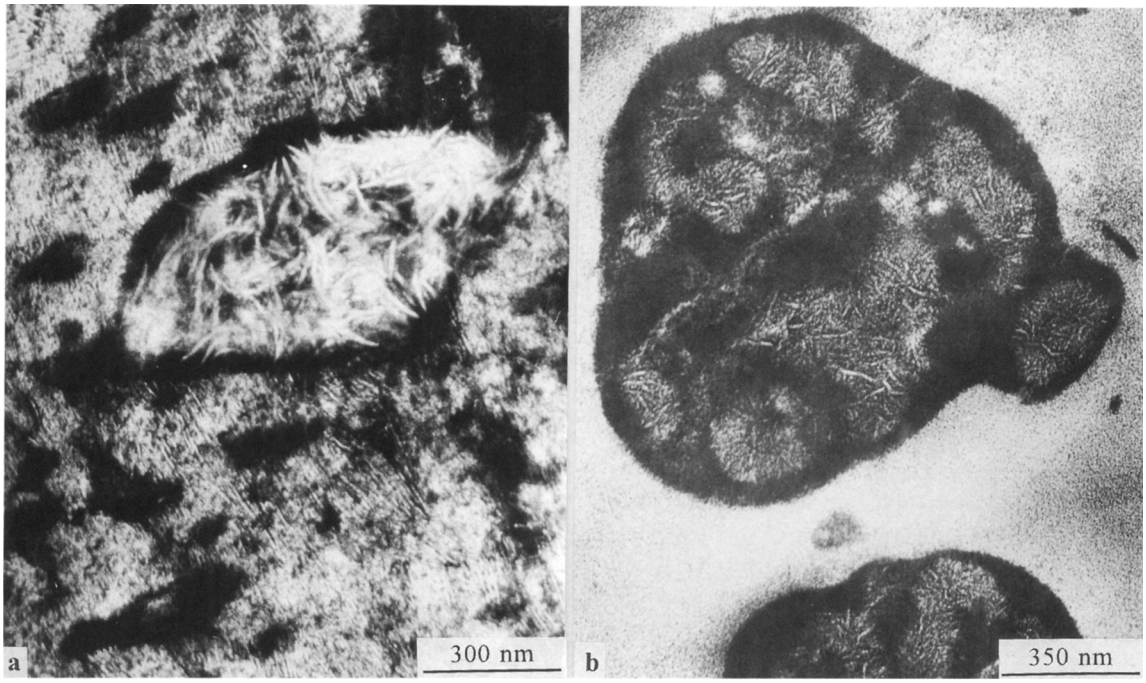

Figure 1 Transmission electron micrographs of the impact modified PP with EPR: (a) EPR particles possessing one inclusion and (b) EPR particles possessing several inclusions.

is visible together with matrix strands between voids. These are strongly plastically stretched, fibrillized, and finally broken down.

Mechanical properties and morphological parameters are summarized in Table I. As shown, the impact strength of sample 2 is significantly greater

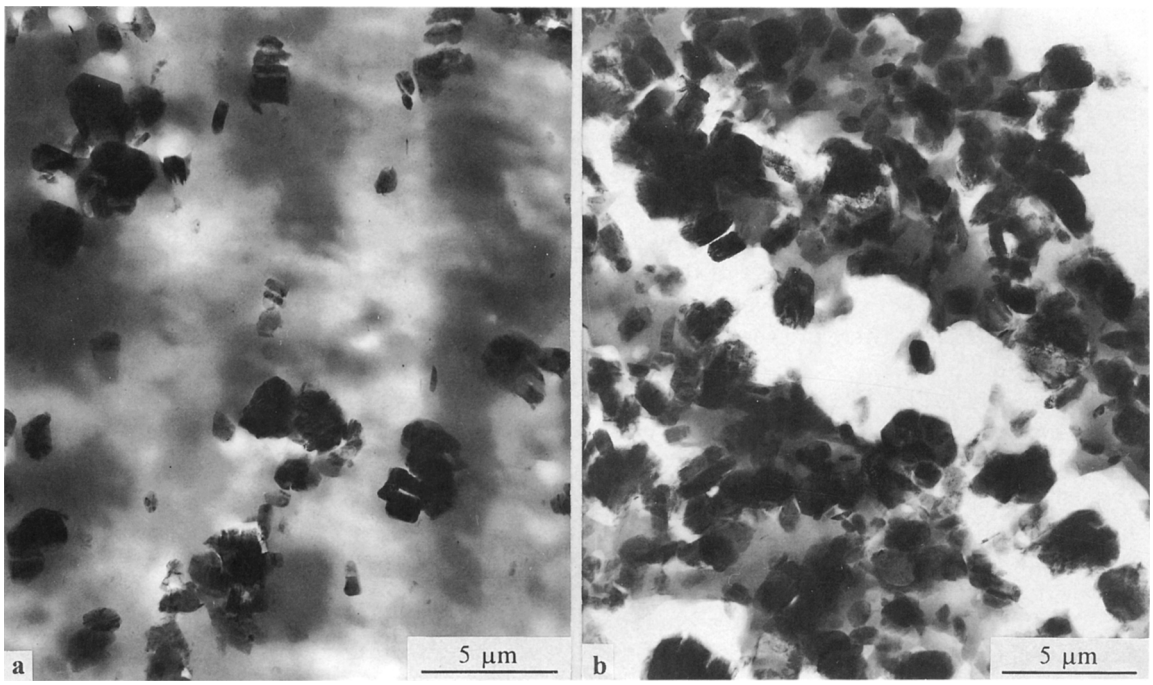

Figure 2 High voltage electron micrographs of the modified PP with Al_2O_3 filler particles: (a) 10 wt % Al_2O_3 filler particles and (b) 60 wt % Al_2O_3 filler particles.

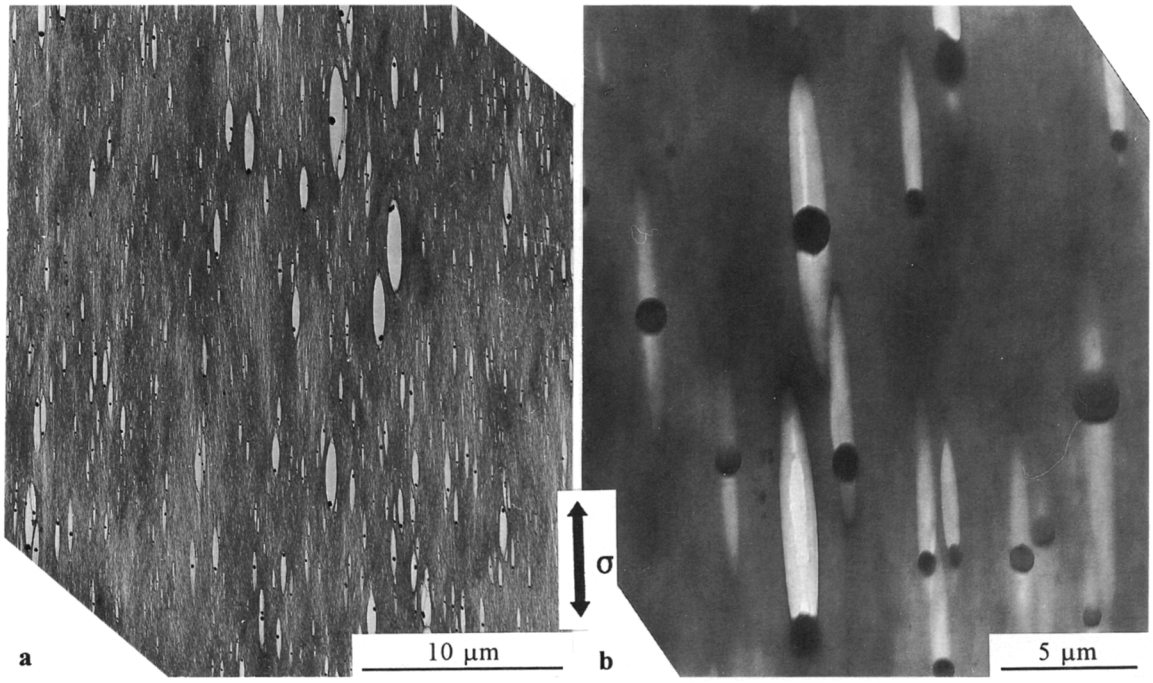

Figure 3 Deformation structures of the impact modified PP with EPR possessing one inclusion. High voltage electron micrographs at (a) low magnification and (b) higher magnification.

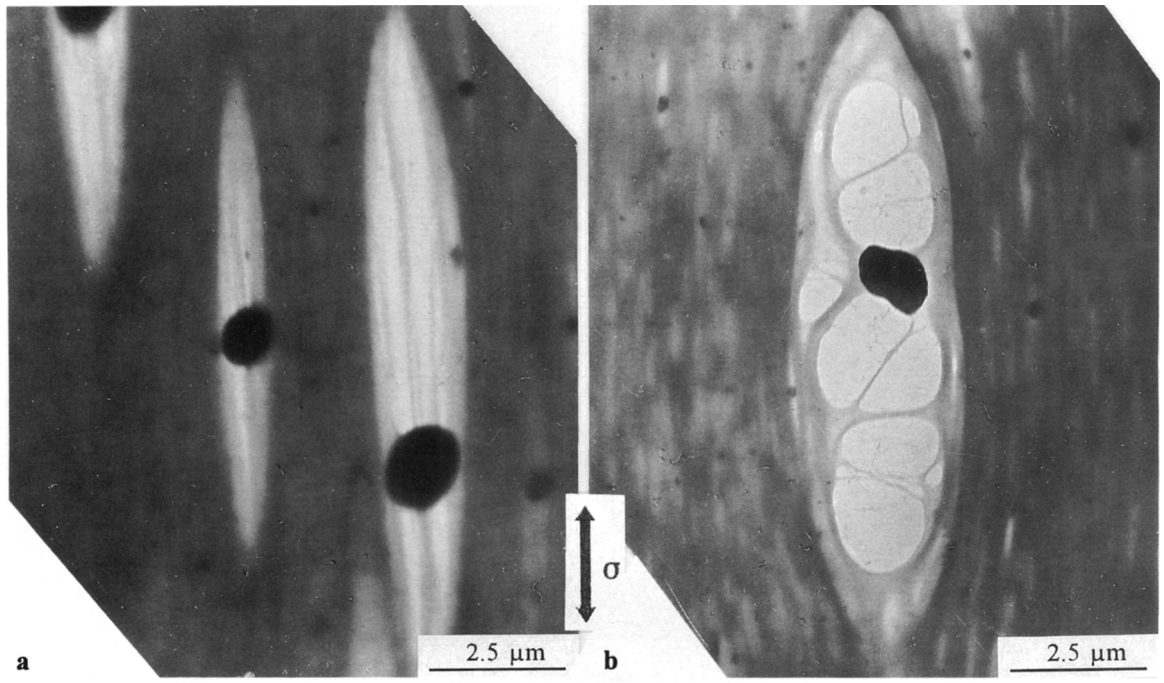

Figure 4 High voltage electron micrographs from the impact modified PP with EPR possessing one inclusion: (a) plastic deformed EPR-rubbery shell and (b) void formation (cavitation) in the EP-rubbery shell.

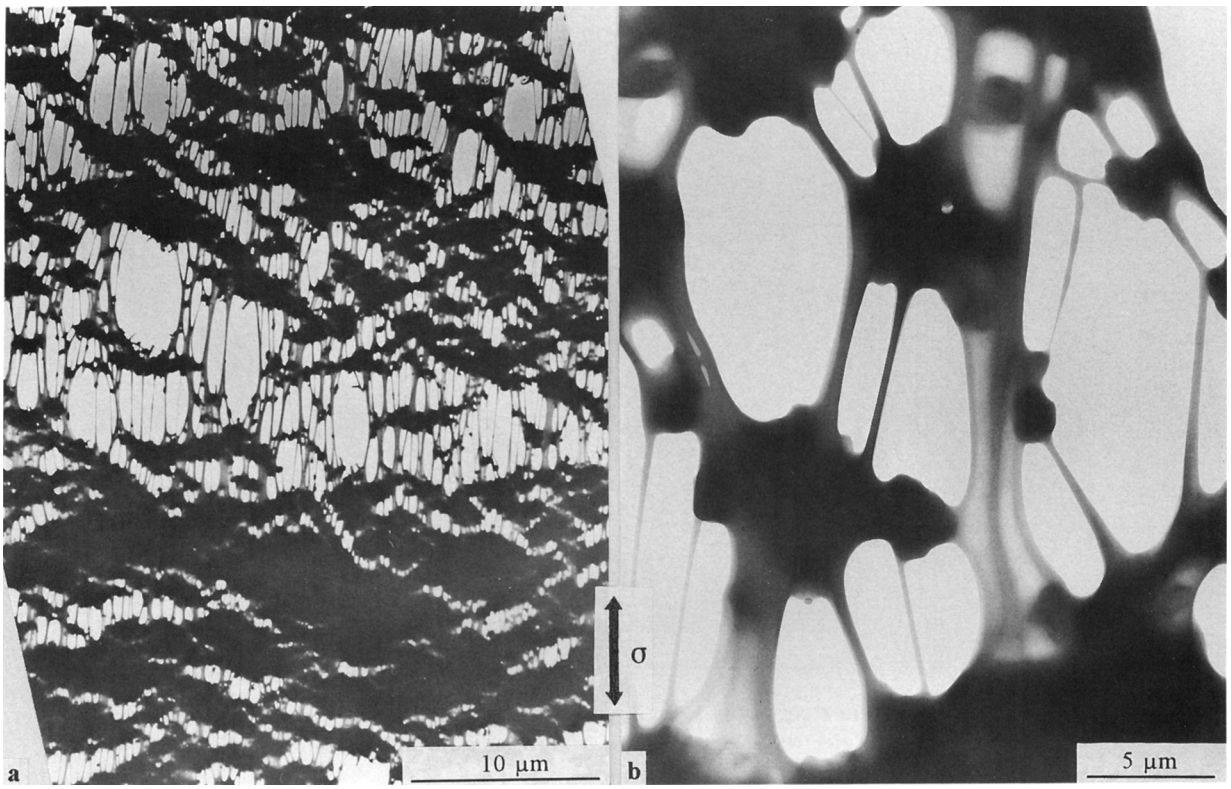

Figure 5 Deformation structures of the impact modified PP with EPR possessing several inclusions. High voltage electron micrographs at (a) low magnification and (b) higher magnification.

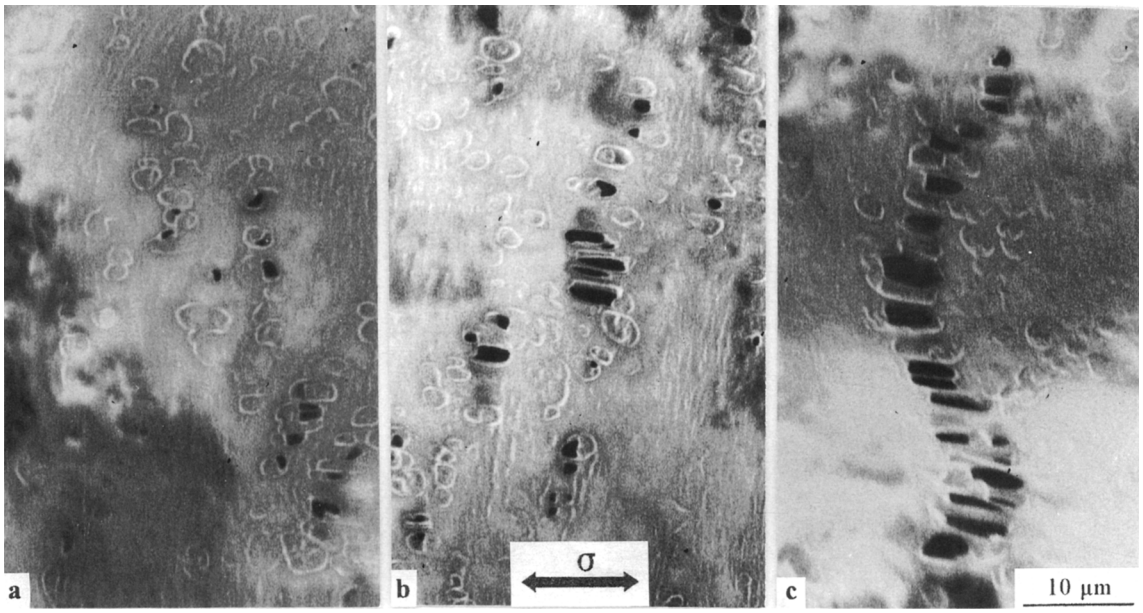

Figure 6 Deformation structures of the impact modified PP with EPR possessing several inclusions at the early stage of deformation in the scanning electron microscope (see text).

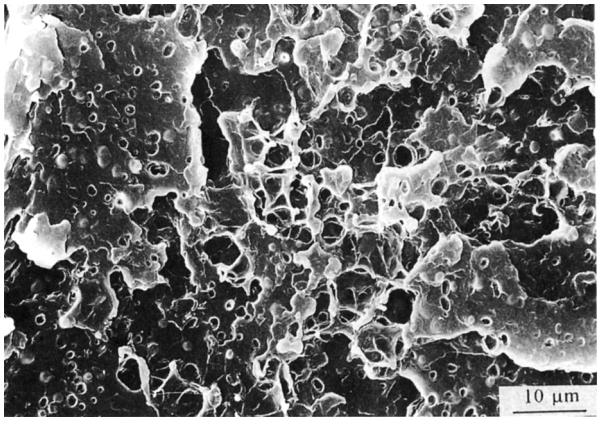

Figure 7 Scanning electron micrograph from the fracture surface where the stress whitening occurred during the tensile test.

than that of sample 1. The reason for this is explained in the Discussion section.

PP Modified with Al_2O_3 Filler Particles

Stress–strain curves of both particle filled PP systems are shown in Figure 8. Sample 3 with 10 wt % Al_2O_3 particles shows a necking phenomenon with a stress–strain curve similar to that of ductile materials.[14] Sample 4 with 60 wt % Al_2O_3 modifier particles deforms without necking, and the stress–strain curve deviates directly after reaching the yield point without change of the stress. There is a remarkable reduction in yield stress for sample 4 as a consequence of a stress field superposition with increasing the weight fraction of filler particles and consequent decreasing of particle distance.

Figure 9 shows successive optical micrographs during the tensile tests. Figure 9(a,b) were taken from sample 3. We can see that at low weight fraction of filler particles the sample deforms homogeneously up to the yield point [Fig. 9(a)]. After that necking occurs [Fig. 9(b)]. A sequence of optical micrographs of deformed sample 4 [see Fig. 9(c,d)] show the development of stress-whitening zones in the form of bands perpendicular to the load direction without formation of necking. With increasing strain, these bands will be extended in the whole scale of the sample. Once this extension was finished, the crack was initiated and consequently the sample failed.

Due to poor adhesion between the Al_2O_3 filler particles and the matrix, the debonding mechanism takes place easily at the both sides of the particles in parallel direction to the applied stress (i.e., at the poles).[15] Sample 3 modified with 10 wt % Al_2O_3 filler particles shows void formation due to debonding with elongation up to 800% in the direction of the applied stress (Fig. 10). If the matrix strands in between the particles are sufficiently large, the contraction of the sample in the direction perpendicular to the applied stress also occurs following necking. In connection with the debonding process, the matrix deforms plastically through shear yielding.

Figure 11 shows the deformation structures of sample 4 with 60 wt % Al_2O_3 filler particles. Here, the void formation appears in bands across the sample with only very thin matrix strands between the particles. Because the stress field interacts very intensively due to the high modifier particle content, a crazelike deformation structure occurs (Fig. 11). The microdeformation process in this sample follows also by void formation due to debonding. However, the matrix deforms plastically through the shear flow process.

DISCUSSION

Model Representation

In the following, the influences of type and structure of modifier particles on the micromechanical deformation processes are discussed in more detail.

Figure 12 shows a schematic representation of phase morphology for the systems modified with EP block copolymer. These systems show a ternary system: because the interfacial stress between the EP phase and the PP matrix is lower than that between the PE phase and the PP matrix, its interface develops as a rubber shell around the PE core.[16]

In general, the average particle size is dependent on the viscosity ratio between the dispersed phase

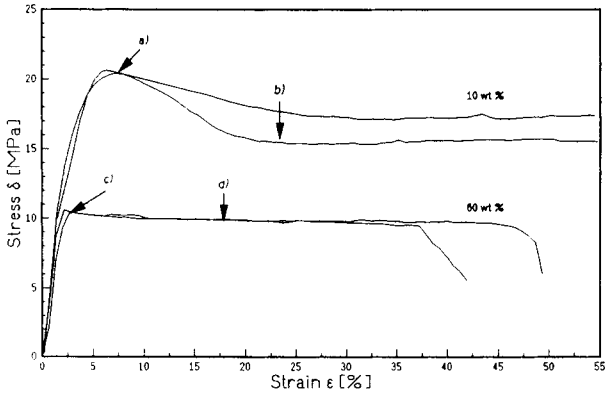

Figure 8 The stress–strain diagram from the uniaxial tensile test of the modified PP with Al_2O_3 filler particles at a crosshead speed of 0.5 mm/min and at 23°C.

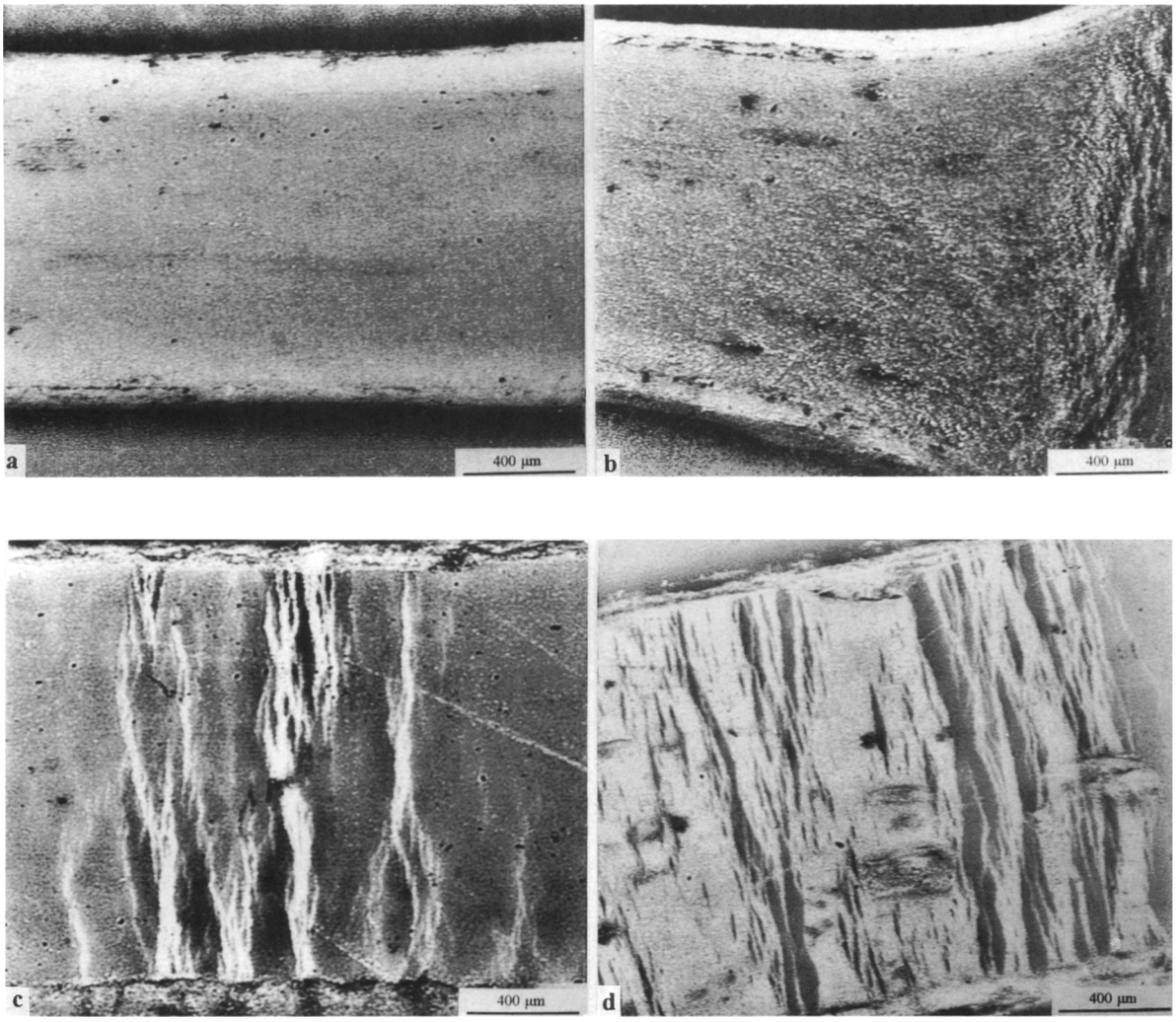

Figure 9 Successive optical micrographs at the points indicated in the stress–strain diagram.

and the matrix.[17–19] This may be correct, only if a particle has one inclusion with a rubbery shell. However, when a particle has several inclusions with a rubbery shell, the final average particle size is not dependent only on viscosity ratio, because the average particle is an aggregation of the individual particles. TEM micrographs (Fig. 1) show that the EP-rubbery phase in sample 1 resides in the PP matrix as a separate phase, whereas in sample 2 there is no indication of the formation of a EP-rubbery separate phase in the PP matrix. In addition, the thickness of the rubbery shell is relatively greater than that in sample 1. However, the size of PE inclusions inside the EPR particles in both samples remain nearly constant. Therefore, we concluded that with higher EPR concentrations, the individual EPR particles aggregate, yielding greater particles with several inclusions.

Figure 13–15 show schematic models of micromechanical deformation processes from the results of the electron microscopic investigation in the form of a three-stage mechanism[16]: stage 1, stress concentration; stage 2, void and shear band formation; and stage 3, shear yielding.

At the beginning of deformation, the modifier particles act as stress concentrators, and the stress field is disturbed by dispersed particles. The stress concentration leads to the development of a triaxial stress in the rubber particles and to a dilatation of the matrix. Elongation of the particles together with the matrix is followed by localized plastic deformation because of the stress concentrations for the systems modified with EPR. In this stage, weak shear bands also occur, because there is a maximum shear stress component under an angle 45°. The deformation processes are initiated in the rubber par-

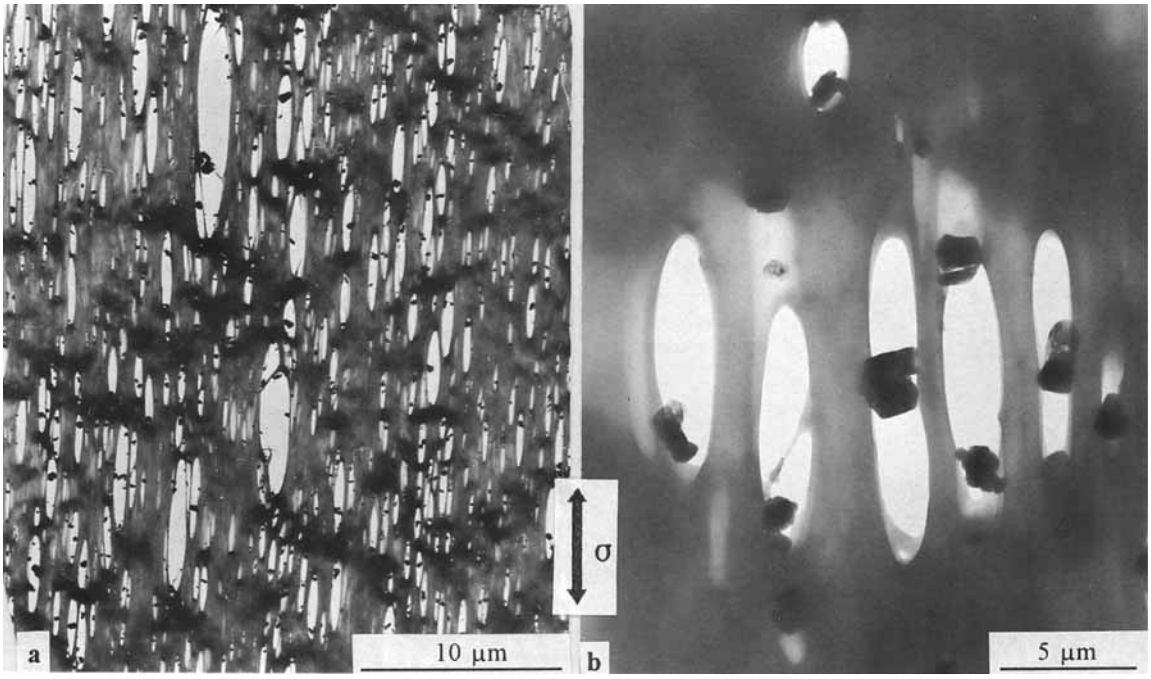

Figure 10 Deformation structures of the modified PP with 10 wt % Al_2O_3 filler particles in the high voltage electron microscope.

ticles and not in the matrix or at the interfaces in systems modified with EPR particles. In the second stage, due to the stress concentration a higher hydrostatic stress builds up inside the particles and gives rise to void formation through cavitation inside the particles for the systems with EPR modifier

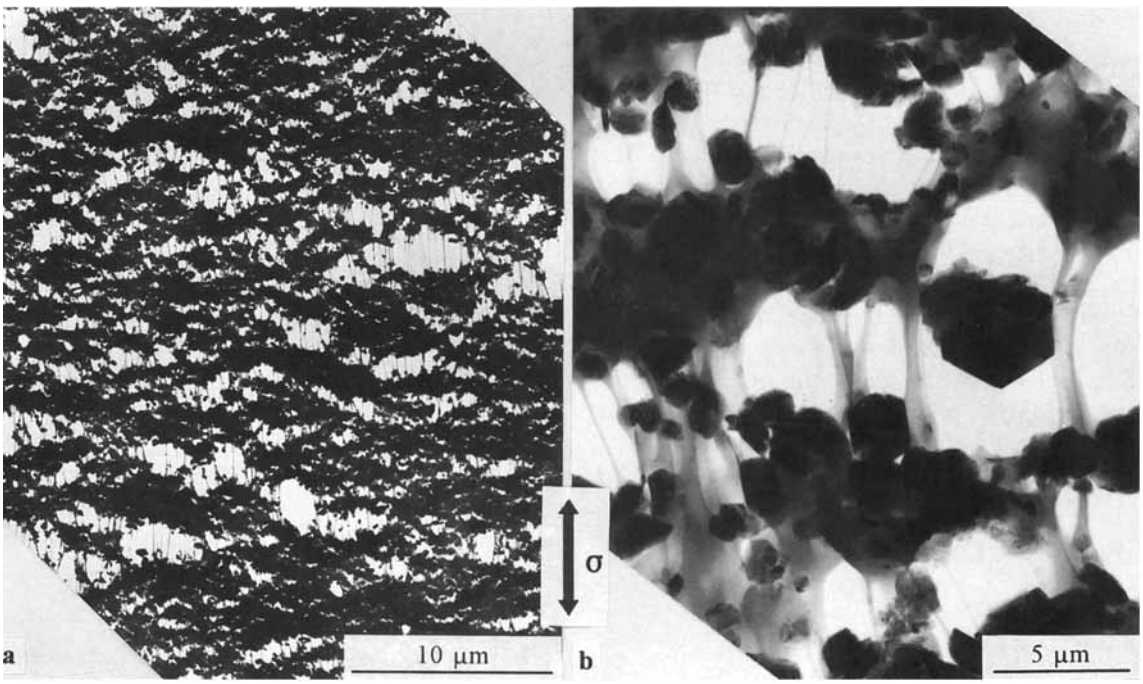

Figure 11 Deformation structures of the modified PP with 60 wt % Al_2O_3 filler particles in the high voltage electron microscope.

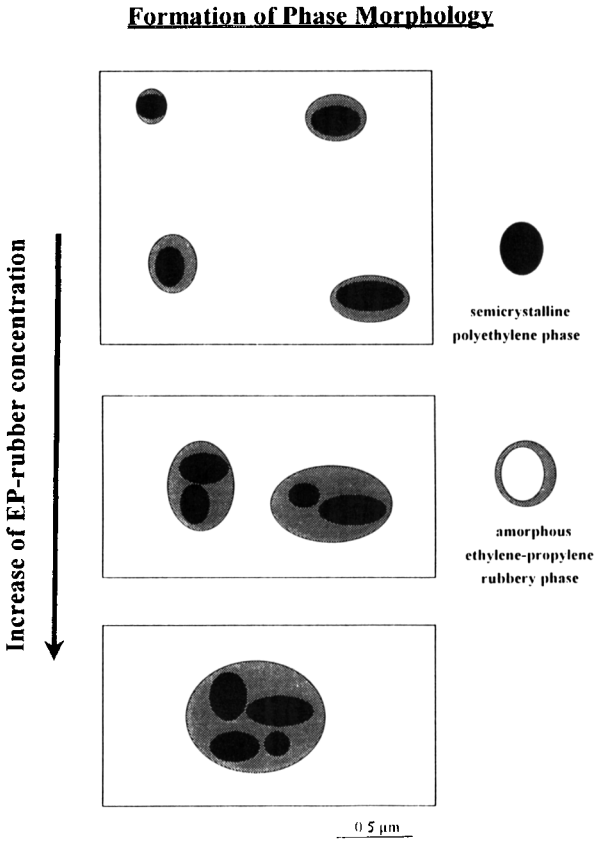

Figure 12 Schematic representation of phase morphology for the systems modified with EPR particles.

particles. Voids form due to debonding at the interface between the rigid filler particles and the matrix in the systems with rigid Al_2O_3 particles. In the third stage, induced shear deformation takes place. The void formation due to cavitation and debonding can dissipate the triaxial tension. After cavitation or debonding the triaxial stress state is locally relieved and the yield strength is lowered. Cavitation of the rubber particles will result in a local decrease in the hydrostatic component of the stress and a corresponding increase in the shear component.[20] Once the void formation is initiated, the further shear yielding is greatly enhanced in the matrix.

COMPARISON OF RESULTS

PP/EPR

Sample 1

Although the EPR particles act as stress concentrators, the *CD/D* value of 6.06 would be too large to initiate the overlapping of stress fields around adjacent particles in the matrix. Therefore, as one can see from Figure 6, weak shear bands form in the matrix between particles. Due to the stress concentration, a higher hydrostatic stress builds up inside the particles; void formation follows by a single cavitation process inside particles, because the particles in this sample possess only one inclusion. However, as the strain is increased above the maximum tensile stress, a local yielding of the matrix occurs due to the rubber induced shear deformation.[17]

Sample 2

The *CD/D* value of 2.34 is small enough for the overlapping of the stress fields around adjacent modifier particles. Thereby voids are easily produced, and the multiple cavitation process takes place in this system, because the EPR particles have several PE inclusions with a EP-rubbery shell. As a consequence, a crazelike structure of deformation is observed (Fig. 4); this was observed also by other authors.[12,21,22] It is noted that the deformation structure seems like a craze, but it is not the same as the craze described in the literature. Toughness

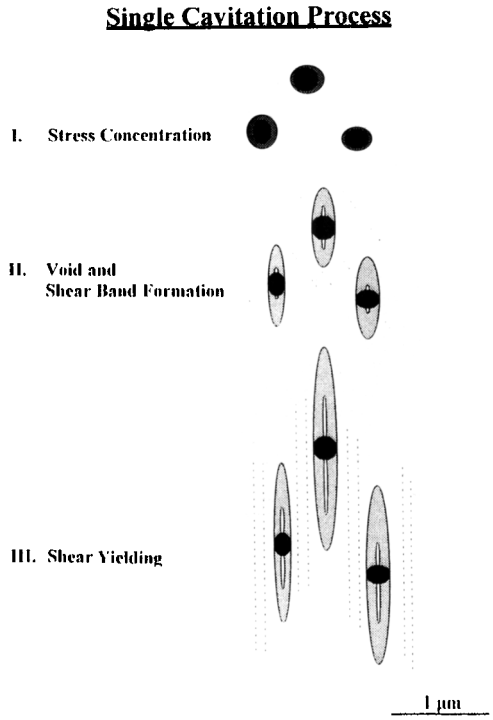

Figure 13 Schematic model of micromechanical deformation process: three-stage mechanism in the impact modified PP with EPR possessing one inclusion following the single cavitation process.

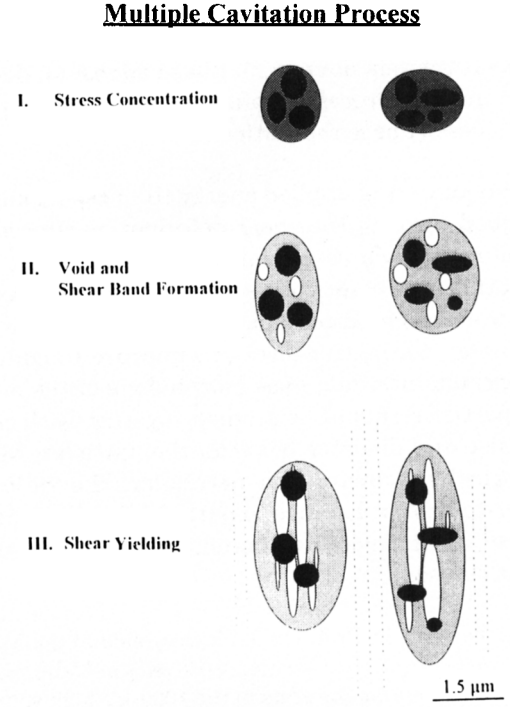

Figure 14 Schematic model of micromechanical deformation process: three-stage mechanism in the impact modified PP with EPR possessing several inclusions following the multiple cavitation process.

of this sample is significantly higher than that of sample 1 (in particular, at the low temperature it is improved by a factor of 4).

PP/Al_2O_3

Sample 3

Large matrix strands between the particles (*CD/D* values are large). Therefore, stress field overlapping cannot take place, and the matrix deforms through shear banding due to debonding processes.

Sample 4

The matrix strands between the particles (i.e., the ratios *CD/D*) are very small. The matrix strands can be strongly plastically fibrillized due to the great influence of the stress field overlapping. Therefore, deformation structure is crazelike (compare Fig. 3 with Fig. 11).

Although the initial deformation processes for systems modified with Al_2O_3 filler particles are different, the deformation structures are very similar to those of the system modified with EPR particles (compare with Figs. 3, 6, 10, and 11). Cavitation and debonding processes in both types of modified PPs could be explained by the formation of dilatation bands, which was suggested by Lazzeri and Bucknall.[23] Until the dilatation bands of voids orient themselves perpendicularly to the axis of the applied stress, the strain increases further. Once the dilatational bands are aligned perpendicularly to the axis of the applied stress, the fibrils break down and the crack develops.

Many investigations demonstrated that the impact toughness might be greatly improved if the interparticle distances are smaller than a critical value.[3,24] At first, the interparticle distance model was developed from the effect of stress field overlapping.[3] The level of impact strength in toughened polymers depends mainly upon the rubber concentration and not on the particle size. Because the interparticle distance is interrelated with the rubber concentration and particle size, only the interparticle distance should not be responsible for the level of impact strength as well as for the micromechanical deformation processes. Therefore, it may be responsible only for the brittle-to-tough transition temperature. In addition, the level of stress concentration is independent on particle diameter; whereas

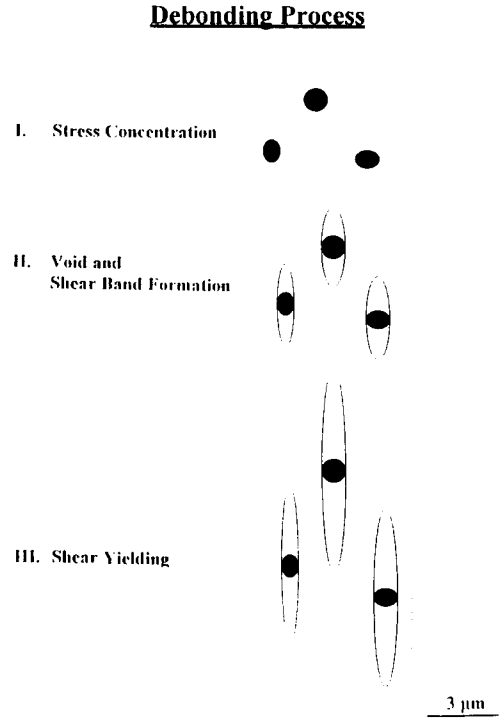

Figure 15 Schematic model of micromechanical deformation process: three-stage mechanism in the impact modified PP with Al_2O_3 filler particles following the debonding process.

the dimension of the stress concentration zone is dependent on particle diameter. Therefore, to study the micromechanical deformation processes, the interparticle distance and the particle size must be considered together. With respect to this, we concentrated in the present work on the effect of the ratio of the center-to-center distance to particle size on the micromechanical deformation processes. If the ratio CD/D is higher than a critical value, the stress fields around adjacent modifier particles do not interact. Therefore, only shear bands appear between particles. If the ratio CD/D is smaller than a critical value, the interaction of particle stress fields yields to higher stresses in the thin matrix strands. Therefore, a crazelike structure of deformation occurs.

In addition, Rümpler et al.[25] suggested that in the PP-*block* copolymer system with high rubber concentration, the EPR particles provide additional impact toughness and improve the stiffness to a small extent. We have evidence from the electron microscopic investigation that the modifier particles with several inclusions are more effective for toughening PP modified with EPR particles. It can be explained clearly that the system modified with several inclusions dissipates more impact energy through multiple cavitation processes than that modified with one inclusion.

Recently, Li and coworkers[26–28] investigated the failure mechanisms of particulate filled thermoplastic polyester. They found that a ductile-to-quasibrittle transition occurred as a function of volume fraction. In our *in situ* tensile tests in an electron microscope, with lower Al_2O_3 filler content the normal ductile deformation structure appeared with neck formation; with higher Al_2O_3 filler content the quasibrittle deformation structure (crazelike) appeared without neck formation. These results are quite consistent with the observations by Li et al.[26–28]

CONCLUSIONS

The micromechanical toughening mechanisms for different modified PP systems were studied. The mechanical properties of toughening modified heterogeneous thermoplastics should be decisively influenced by the morphology of modified particles. Micromechanical deformation processes could be determined as following:

1. If there is a phase adhesion between the modifier particles and the matrix, deformation processes follow by either a multiple or single cavitation process.
2. If there is poor or no phase adhesion, deformation processes follow by a debonding process (phase separation).

The major part of applied energy to the specimen is absorbed through the shear deformation processes in the matrix via cavitation processes, that is, the cavitation processes themselves are not the major energy absorbing mechanisms, but they provide for the energy dissipating sites. To improve toughness the optimal internal phase morphology of the modifier particles should be studied together with particle size and distance between the particles. Morphological parameters, in particular, the ratio of center-to-center distance to particle diameter, have a great significance for micromechanical deformation processes.

The authors thank Prof. Dr. J. Heydenreich of the Max-Plank-Institute of Microstructure-Physics in Halle/Salle for allowing deformation tests in the 1000-kV high voltage electron microscope, and the members of the HVEM group, Ch. Dietzsch, E. Hunold, and W. Greie for technical help. We thank Mrs. I. Dubnikova of the Institute of Chemical Physics of Russian Academy of Sciences in Moscow for preparing the Al_2O_3 filled PPs. We also gratefully thank the Deutsche Forschungsgemeinschaft (Graduiertenkolleg "Heterogene Polymere") and the Max-Buchner-Forschungsstiftung for financial support of G.-M. K.

REFERENCES

1. C. B. Bucknall, *Toughened Plastics,* Applied Science, London, 1977.
2. J. N. Goodier, *J. Appl. Mech. (Trans. ASME),* **55,** 39 (1933).
3. S. Wu, *Polymer,* **26,** 1855 (1985).
4. R. J. M. Borggreve, R. J. Gaymans, and H. M. Eichenwald, *Polymer,* **30,** 78 (1989).
5. S. Y. Hobbs, R. C. Bopp, and V. H. Watkins, *Polym. Eng. Sci.,* **23,** 380 (1983).
6. H. Sue and A. F. Yee, *J. Mater. Sci.,* **24,** 1447 (1989).
7. G. H. Michler and K. Gruber, *Plaste Kautschuk,* **23,** 346 (1976).
8. G. H. Michler, *Kunststoff-Mikromechanik: Morphologie, Deformations, und Bruchmechanismen,* Carl Hanser Verlag, München/Wien, 1992.
9. G. H. Michler, *Acta Polym.,* **36,** 285 (1985).
10. S. Wu, *J. Appl. Polym. Sci.,* **35,** 549 (1988).
11. G. H. Michler and J. M. Tovmasyan, *Plaste Kautschuk,* **35,** 35 (1988).
12. F. Ramsteiner, G. Kanig, W. Heckmann, and W. Gruber, *Polymer,* **24,** 365 (1983).

13. P. Galli, J. C. Haylock, and T. Simonazzi, in *Manufacturing and Properties of PP Copolymers, Polypropylene—Structure, Blends and Composites,* Vol. 2, J. Karger-Kocsis, Ed., Chapman & Hall, London, 1995, p. 1.
14. P. H. Th. Vollenberg and D. Heikens, *J. Mater. Sci.,* **25,** 3089 (1990).
15. A. J. Kinloch and R. J. Young, *Fracture Behaviour of Polymers,* Applied Science, London, 1983.
16. G. H. Michler, *Acta Polym.,* **44,** 113 (1993).
17. F. C. Stehling, T. Huff, and S. Speed, *J. Appl. Polym. Sci.,* **26,** 2693 (1981).
18. S. Wu, *Polym. Eng. Sci.,* **27,** 335 (1987).
19. S. Y. Hobbs, M. E. J. Dekkers, and V. H. Watkins, *Polymer,* **29,** 1598 (1988).
20. C. B. Bucknall, P. S. Heather, and A. Lazzeri, *J. Mater. Sci.,* **16,** 2255 (1989).
21. C. J. Chou, K. Vijayan, D. Kirby, A. Hiltner, and E. Baer, *J. Mater. Sci.,* **23,** 2521 (1988).
22. R. C. Cieslinski, *Proceedings of the Cambridge Conference 1994: Deformation, Yield and Fracture of Polymers,* Cambridge, U.K., April 1994.
23. A. Lazzeri and C. B. Bucknall, *J. Mater. Sci.,* **28,** 6799 (1993).
24. R. J. M. Borggreve and R. J. Gaymans, *Polymer,* **29,** 1441 (1988).
25. K.-D. Rümpler, J. F. R. Jaggard, and R. A. Werner, *Kunststoffe,* **78,** 602 (1988).
26. S. Bazhenov, J. X. Li, A. Hiltner, and E. Baer, *J. Appl. Polym. Sci.,* **25,** 243 (1994).
27. J. X. Li, M. Silverstein, A. Hiltner, and E. Baer, *J. Appl. Polym. Sci.,* **25,** 255 (1994).
28. J. X. Li, A. Hiltner, and E. Baer, *J. Appl. Polym. Sci.,* **25,** 269 (1994).

Received July 10, 1995
Accepted October 27, 1995